Inulin-based polymer coated SPIONs as potential drug delivery systems for targeted cancer therapy

UNIVERSITÀ DEGLI STUDI DI TORINO

Inulin-based polymer coated SPIONs as potential drug delivery systems for targeted cancer therapy

C. Scialabba, M. Licciardi, N. Mauro, F. Rocco, M. Ceruti, G. Giammona

Abstract

This paper deal with the synthesis and characterization of PEGylated squalene-grafted-inulin amphiphile capable of self-assembling and self-organizing into nanocarriers once placed in aqueous media. It was exploited as coating agent for obtaining doxorubicin loaded superparamagnetic iron oxide nanoparticles (SPIONs) endowed with stealth like behavior and excellent physicochemical stability. Inulin was firstly modified in the side chain with primary amine groups, followed in turn by conjugation with squalenoyl derivatives through common amidic coupling agents and PEGylation by imine linkage. Polymer coated SPIONs were so obtained by spontaneous self-assembling of inulin copolymer onto magnetite surface involving hydrophobic–hydrophobic interactions between the metallic core and the squalene moieties. The system was characterized in terms of hydrodynamic radius, zeta potential, shape and drug loading capacity. On the whole, the stealth-like shell stabilized the suspension in aqueous media, though allowing the release of the doxorubicin loaded in therapeutic range. The cytotoxicity profile on cancer (HCT116) cell line and in vitro drug uptake were evaluated both with and without an external magnetic field used as targeting agent and uptake promoter, displaying that magnetic targeting implies advantageous therapeutic effects, that is amplified drug uptake and increased anticancer activity throughout the tumor mass.

Introduction

Therapeutic approaches used to eradicate tumors involve invasive processes, long term largely ineffective, such as surgical removal of neoplastic mass [1]. The surgical therapy often needs further treatments during the follow-up, encompassing chemotherapy or radiotherapy [2]. The latter, even though it is the most localized technique, entails several drawbacks, among which, repeated treatments and secondary effects (e.g., sterility and side tumor genesis) [3]. In addition, current chemotherapy fails in many cases because of the recurrence of metastases or heavy toxic effects. These therapeutic limitations are mainly due to the lack of selective drug accumulation into the tumor site, thus affecting healthy cells as well [4] and [5]. The use of nanocarriers, designed to enhance drugs efficiency, permits to overcome some of these matters being drugs released into a specific body district. Several systems have been developed so as to act as drug delivery systems useful for targeted therapy, such as polymeric micelles [6], [7] and [8] liposomes [9], polymersomes [10], polymeric nanoparticles [11] and [12], and magnetic nanoparticles [1].

Magnetic nanoparticles represent an innovative class of nanocarrier which has proved capable of targeting anticancer drugs, avoiding the most part of limitations attributable to conventional therapeutic tools. Such systems imply improved bioavailability in the tumor site by means of a double targeting effect, namely enhanced permeability retention effect (EPR) [13] and [14] (passive) and the magnetic targeting owing to the attraction to an external magnetic field. The advantages above

reported lead to other benefits, including reduced toxicity toward healthy cells and the ability to locally deliver a high drug payload into tumor mass. Superparamagnetic iron oxide nanoparticles (SPIONs) are a unique family of magnetic nanoparticles endowed with additional advantageous physicochemical properties. Specifically, they show magnetic interactions that do not persist once the external magnetic field is removed (superparamagnetism) [15], and hence site specific magnetic targeting can be efficiently obtained applying onto the tumor mass removable and nontoxic magnetic fields as external drawing force.

SPIONs consist of a solid core made up of iron oxides (magnetite, Fe_3O_4 and/or maghemite, Fe_2O_3) mostly coated with biocompatible polymers. Typically, the coating agent plays a double role, which is to protect nanoparticles from oxidation and increase their stability when dispersed in aqueous media. Indeed, the presence of a hydrophilic shell avoids hydrophobic–hydrophobic interactions that provoke SPIONs aggregation, so nullifying all advantages related to the nanomeric dimensions of the starting carrier [16]. Many natural and synthetic polymers such as poly(hydroxyethyl) aspartamide derivative [17] and [18], chitosan, ethyl cellulose, poly(lactide) acid, poly(lactide-co-glycolide) acid and poly(ethylene)glycol have been employed as coating agents for enhancing SPIONs stability and conferring surface functional groups available for further reactions [19] and [20]. However, some of these either are not sufficiently bioeliminable or degrade to acidic products often yielding to local inflammation. Therefore, new cost-effective polymers provided with excellent biocompatibility and versatility should be synthesized and studied in view of clinical applications [20], [21] and [22].

In this study we propose inulin-based copolymer as coating agent for SPIONs. Inulin is a natural, biocompatible, bioeliminable and biodegradable [23] polysaccharide consisting of linear chains of β-(2-1) fructose units and typically has a glucose unit attached at the reducing end. It is water soluble and exhibits high hydroxyl functional groups available for common coupling reactions [24]. Various studies have dealt with its chemical modification in order to obtain biocompatible drug delivery systems (DDS), including hydrogels [25], nanoparticles [26], micelles [6] and [27], and macromolecular bioconjugates [28]. Being inulin versatile and highly functionalizable [29] and [30], here we focused our attention on the synthesis of an amphiphilic inulin derivative capable of coating SPIONs once placed in aqueous media. We demonstrated that the polymer-coated SPIONs loaded significant amounts of doxorubicin during the self-assembling process, which was released at physiological conditions in a controlled fashion so acting as an excellent anticancer system. Under the effect of external magnetic stimuli, it was also assessed the ability of the system to be accumulated into a specific area mimicking its potential targeting effect in the human body.

2. Experimental part

2.1. Materials and methods

Squalene (purity > 99%) was purchased from VWR (Italy). Inulin-(2-aminoethyl)-carbamate (INU-EDA), used as starting copolymer, was synthesized as previously reported [6]. Inulin, triethylamine (TEA), ethylenediamine (EDA), Bis(4-nitrophenyl)carbonate (BNPC), doxorubicin hydrochloride (DOXO-HCl), iron oxide (Fe_3O_4) magnetic nanoparticles (10 ± 1 nm) in water, iron(III)chloride,

ferrozine (3-(2-pyridyl)-5,6-bis(phenyl sulfonic acid)-1,2,4-triazine), and neocuproine (2,9-dimethyl(1,10-phenanthroline)), were purchased from Aldrich (Milan, Italy). N-hydroxysuccinimide (NHS), 1-ethyl-3-(3-dimethylaminopropyl)-carbodiimide hydrochloride (EDC-HCl), O-[2-(6-oxocaproylamino)-ethyl]-O′-methylpolyethylene glycol 2000 (PEG-CH═O), Sephadex G-15, anhydrous dimethylformamide (DMF), were purchased from Fluka (Switzerland). All reagents were of analytic grade, unless otherwise stated. SpectraPor dialysis tubing was purchased from Spectrum Laboratories, Inc. (Italy).

The ^{1}H NMR spectra were recorded using a Bruker Avance II 300 spectrometer operating at 300 MHz. Fluorescence spectroscopy was performed by using a Shimadzu RF-5301 PC spectrofluorimeter. Centrifugations were performed using a Centra MP4R IEC centrifuge. Size exclusion chromatography (SEC) was carried out using a Phenomenex PolySep-GFC-P3000 column (California, USA) connected to a Water 2410 refractive index detector. Phosphate buffer pH 6.5/methanol 9:1 (v/v) solution was used as eluent at 35 °C with a flux of 0.6 mL/min, and pullulan standards (112.0–0.18 kDa, Polymer Laboratories Inc., USA) were used to set up calibration curve.

2.2. Synthesis of 1,1′,2-tris-nor-squalene acid (SqCOOH-C27): (4E,8E,12E,16E)-4,8,13,17,21-pentamethyl-4,8,12,16,20-docosapentaenoic acid

1,1′,2-Tris-nor-squalene aldehyde [31], [32] and [33] (1.58 g, 4.12 mmol) was dissolved in diethyl ether (20 mL) at 0 °C. Separately, sulfuric acid (2.3 mL) was added at 0 °C to distilled water (20 mL) with stirring, followed by potassium dichromate (1.21 g, 4.12 mmol) to obtain chromic acid. It was then added at 0 °C within 20 min to the solution of 1,1′,2-tris-nor-squalene aldehyde, previously prepared, and left to react for 2 h at 0 °C with stirring. The reaction mixture was extracted with diethyl ether (50 mL × 3), washed with saturated brine, dried over anhydrous sodium sulfate and evaporated in vacuum. The completion of the reaction was revealed by silica gel TLC with light petroleum/diethyl ether/methanol, 70:23:7. The crude product was purified by flash chromatography with light petroleum, then light petroleum/diethyl ether, 95:5 as eluent, to give 578 mg of 1,1′,2-tris-nor-squalene acid (35% yield), as a colorless oil.

^{1}H NMR spectra were recorded on a Bruker 300 ultrashield instrument (Karlsruhe, Germany) for samples in $CDCl_3$ solution at room temperature, with Me_4Si (TMS) as internal standard. Coupling constants (*J*) are given in Hz. Mass spectra were recorded on a Finnigan MAT TSQ 700 spectrometer (San Jose, CA). The reactions were monitored by TLC on F_{254} silica gel precoated sheets (Merck, Damstadt, Germany); after development, the sheets were exposed to iodine vapor. Flash-column chromatography was performed on 230–400 mesh silica gel.

^{1}H NMR ($CDCl_3$): δ, 1.55–1.63 (m, 18 H, allylic CH_3), 1.90–2.05 (m, 16 H, allylic CH_2), 2.26 (t, 2 H, C**H**$_2$CH$_2$COOH), 2.38 (t, 2 H, CH$_2$C**H**$_2$COOH), 5.00–5.19 (m, 5 H, vinylic CH), 12.20 (broad, 1 H, COOH). MS (EI): *m/z* 400 (M+, 5), 357 (3), 331 (5), 289 (3), 208 (6), 136 (3), 81 (100).

2.3. Synthesis of Inulin-1,1′,2-tris-nor-squalene (INU-Sq)

SqCOOH-C_{27} (12 mg, 1.5 × 10^{-2} mmol) was solubilized in DMF (1.2 mL), and then EDC-HCl (3.6 mg, 1.9 × 10^{-2} mmol) was added. After that, NHS (2.2 mg, 1.9 × 10^{-2} mmol) and TEA (3 µL, 2.1 × 10^{-2} mmol)

were added to the reactive mixture at once together and the reaction was kept 4 h at 40 °C. The resulting solution was added to 4 mL of a INU-EDA solution in DMF (25 mg/mL) drop-wise and left to react at 25 °C for 18 h. The INU-Sq conjugate was then precipitated in diethyl ether/dichloromethane mixture (2:1 vol/vol) and collected by centrifuging at 5 °C for 5 min, at 9000 rpm. The solid residue was then washed four times with the same mixture. The obtained solid product was dried under vacuum and weighted. INU-Sq was obtained with a yield of 95% (w/w) based on the starting inulin. The obtained copolymer was characterized by ^{1}H NMR (300 MHz, D_2O/DMF-d_7 (5:1): δ 1.12–1.52 (18H, squalenoyl allylic CH_3), 1.91–2.21 (16H, squalenoyl allylic CH_2), 2.9–3.1 ($4H_{EDA}$, —NH—C**H**$_2$—C**H**$_2$—NH—), 3.55–4.0 ($5H_{INU}$, —C**H**$_2$—OH; —C**H**—CH$_2$—OH; —C—C**H**$_2$—O—), 4.02–4.19 ($2H_{INU}$, —C—C**H**—OH; —C**H**—OH).

2.4. Synthesis of = inulin-1,1′,2-tris-nor-squalene-PEG2000 (INU-Sq-PEG2000) graft copolymer

PEG-CHO (21 mg, 1.05×10^{-2} mmol) was added to 4 mL of INU-Sq aqueous solution (22.5 mg/mL) at pH 6.8. The pH of the reaction mixture increased slowly, and consequently the pH of the reaction was kept at 6.8 using 0.1 N hydrochloric acid. The mixture was left with stirring at room temperature overnight. Then it was dried by vacuum and the crude reaction was washed up with diethyl ether/dichloromethane mixture 2:1 vol/vol (4 × 40 mL). The solid product was dried under vacuum yielding a white solid. Yield 85% with respect to the starting inulin. The obtained graft copolymer was characterized by ^{1}H NMR (300 MHz, D_2O/DMF-d_7 (2:1): δ 1.12–1.53 (18H, squalenoyl allylic CH_3), 1.96–2.22 (16H, squalenoyl allylic CH_2), 2.93–3.07 ($4H_{EDA}$, NHC**H**$_2$C**H**$_2$NH), 3.65 ($176H_{PEG2000}$, OC**H**$_2$C**H**$_2$O), 3.67–3.88 ($5H_{INU}$, C**H**$_2$OH; C**H**CH$_2$OH; CC**H**$_2$O), 3.90–4.20 ($2H_{INU}$, CC**H**OH; C**H**OH).

2.5. Preparation of INU-Sq-PEG2000 coated SPIONs (IC-SPIONs)

To an aqueous suspension of Fe_3O_4 (5 mg/mL) INU-Sq-PEG_{2000} copolymer (50 mg) was added with gentile stirring. The obtained mixture was sonicated in an ultrasonic bath for 10 min, thus diluted to 5 mL with double distilled water and, finally, placed into dialysis tube (Spectra Por, Float-A-Lyzers) with a nominal molecular weight cut-off (NMWCO) 8–10 kDa. After 48 h IC-SPIONs were freeze-dried and obtained as a brownish powder. Yield 100%.

2.6. Preparation of doxorubicin loaded IC-SPIONs (Doxo-IC-SPIONs)

Analogous procedure was adopted for the preparation of doxorubicin loaded magnetic nanoparticles (Doxo-IC-SPIONs). For the drug loading, 1 mL of an aqueous doxorubicin hydrochloride solution (10 mg/mL, 1.7×10^{-2} mmol), previously treated with TEA (10 µL, 7×10^{-2} mmol), was added to the polymer/Fe_3O_4 mixture before starting the sonication. The obtained mixture was sonicated in an ultrasonic bath for 10 min and then placed into dialysis tube (Spectra Por, Float-A-Lyzers) with a nominal molecular weight cut-off (NMWCO) 8–10 kDa. After 48 h Doxo-IC-SPIONs were freeze-dried and obtained as a brownish powder. Yield 70%.

2.7. Characterization of the nanosystems

2.7.1. Scanning electron microscopy (SEM)

For the morphology studies, freeze-dried IC-SPIONs were visualized using a scanning electron microscope, ESEM Philips XL30. Samples were dusted on a double sided adhesive tape previously applied on a stainless steel stub. The IC-SPIONs were then sputter-coated with gold prior to microscopy examination.

2.7.2. Dynamic Light Scattering (DLS) measurement and Z-potential analysis

DLS studies and *Z*-potential measurements (mV) were performed at 25 °C using a Malvern Zetasizer NanoZS instrument, fitted with a 532 nm laser at a fixed scattering angle of 173°. Aqueous solutions of IC-SPIONs and Doxo-IC-SPIONs (0.2 mg/mL), were analyzed after filtration through a 5 µm cellulose membrane filter. The intensity-average hydrodynamic diameter and polydispersity index (PDI) were obtained by cumulants analysis of the correlation function. The zeta potential (mV) was calculated from the electrophoretic mobility using the Smoluchowski relationship and assuming that$K \cdot a \gg 1$ (where K and a are the Debye–Hückel parameter and particle radius, respectively).

2.7.3. FT-IR analysis

Investigation of the general and quantitative composition of polymer coated iron oxide nanoparticles were carried out via infrared spectroscopy (FT-IR). The spectra of INU-Sq-PEG_{2000} copolymer, IC-SPIONs and solid SPIONs were recorded in KBr pellets in the frequency range of 4000–400 cm^{-1} by using a Perkin-Elmer Spectrum RX I FT-IR system spectrophotometer. Spectra were recorded in transmittance scale (%*T*) with a resolution of 1 cm^{-1} and a number of scans = 100.

2.7.4. Total iron determination

The iron content in IC-SPIONs and Doxo-IC-SPIONs was measured using the Ferrozine-based spectrophotometric iron estimation method [17]. For this method freeze-dried IC-SPIONs (5 mg) or Doxo-IC-SPIONs (5 mg) were dispersed in 1.4 N hydrochloric acid (1 mg/mL) and kept for 2 h at 60 °C in a water bath to allow the disaggregation of nanoparticles and complete dissolution of the Fe_3O_4 nanoparticles. After that, 1 mL of iron-detection reagent (6.5 mM ferrozine, 6.5 mM neocuproine and 1 M acid ascorbic dissolved in acetate buffer at pH 4.5) was added to the iron solution and incubated for 30 min at room temperature. Then, the optical density of the sample was measured at 560 nm using a Shimadzu UV-2401PC spectrophotometer, and the concentration of Fe_3O_4 was calculated by comparing this value with a calibration curve obtained by recording the absorbance of $FeCl_3$ standard solutions (ranging from 0.5 to 5 µg/mL). Water with iron-detection reagent was used as blank.

2.7.5. Determination of drug payload into Doxo-IC-SPIONs and drug release studies

The amount of doxorubicin loaded into Doxo-IC-SPIONs was determined by UV spectroscopy measuring the absorbance at 480 nm of the sample, prepared by dispersing known amounts of these in double distilled water at pH ~ 6. A calibration curve was obtained for serially diluted concentrations of doxorubicin hydrochloride in bidistilled water at pH ~ 6. The content of drug loaded into the system was expressed as the amount of loaded doxorubicin per unit mass of dry nanoparticles, and resulted to be 11.6 ± 0.5% (w/w), while the encapsulation efficiency was calculated to be 58.5%.

For drug release studies, an appropriate amount of freeze dried Doxo-IC-SPIONs (5 mg) was suspended in PBS at pH 7.4 (5 mL) and placed into floating dialysis tubing with a MWCO 1 kDa. This dialysis membrane was immersed into PBS at pH 7.4 (15 mL) and incubated at 37 °C under continuous stirring (100 rpm) in a Benchtop 808C Incubator Orbital Shaker model 420, for 48 h. At scheduled time intervals, aliquots of the external medium (1 mL) were withdrawn from the outside of the dialysis membrane and replaced with equal amount of fresh medium. The withdrawn samples were analyzed by HPLC in order to determine the released drug. Profile releases were determined by comparing the amount of released drug as a function of incubation time with the total amount of drug loaded into the Doxo-IC-SPIONs. The same analysis was carried out using PBS at pH 5.5. All release data were compared with the diffusion profile of doxorubicin hydrochloride alone (0.62 mg) obtained by using the same procedure.

Data were corrected taking in account the dilution procedure. Each experiment was carried out in triplicate and the results were in agreement within ±5% standard error.

2.8. Cytotoxicity assay on human colon cancer (HCT116) cells

The cytotoxicity was assessed by the MTS assay on human colon cancer (HCT116) cell lines (purchased from *Istituto Zooprofilattico Sperimentale della Lombardia e dell' Emilia Romagna*, Italy), using a commercially available kit (Cell Titer 96 Aqueous One Solution Cell Proliferation assay, Promega). Cells were seeded in 96 well plate at a density of 2.5×10^4 cells/well and grown in Dulbecco's Minimum Essential Medium (DMEM) with 10% FBS (fetal bovine serum) and 1% of penicillin/streptomycin (10,000 U/mL penicillin and 10 mg/mL streptomycin) at 37 °C in 5% CO_2 humidified atmosphere. After 24 h the medium was replaced with 200 µL of fresh culture medium containing empty IC-SPIONs and Doxo-IC-SPIONs at a concentration per well equal to 0.13, 0.27, 0.54, 0.81 and 1.08 mg/mL, corresponding to 25, 50, 100, 150 and 200 µM of doxorubicin. Moreover, the same experiment was performed applying a permanent magnets (attraction force of 250 g) at the bottom of the wells, and using a concentration of empty IC-SPIONs and Doxo-IC-SPIONs of 0.27 mg/mL (equivalent to 50 µM of doxorubicin). Additionally, cells treated with the same magnet were used as negative control for exposition to external magnetic field. After 24 and 48 h, DMEM was replaced with 100 µL of fresh medium, and 20 µL of a MTS solution was added to each well.

Plates were incubated for additional 2 h at 37 °C. Then, the absorbance at 490 nm was measured using a microplate reader (Multiskan, Thermo, UK). Doxorubicin hydrochloride solutions at the same concentrations were used as a positive control, as pure cell medium was used as a negative control. Results were expressed as percentage reduction of the control cells. All culture experiments were performed in triplicates.

2.9. Cell drug uptake studies

The cellular uptake of the Doxo-IC-SPIONs was evaluated by fluorescence microscopy analysis (Zeiss "AXIO Vert. A1" Microscope Inverted). HCT116 cell line, 2.5×10^4 cells/well, maintained in normal medium were cultured in a 46 well plate at 37 °C in an atmosphere of 5% CO_2 for 24 h. After 24 h the medium was replaced with 200 µL of fresh culture medium containing Doxo-IC-SPIONs or free doxorubicin hydrochloride at final drug concentration of 50 µM, and thus cells were incubated for 4, 24 and 48 h. This experiment was performed with or without an external magnetic field. For the experiments in the presence of an external magnetic field, permanent magnets with an attraction force of 250 g, were fixed to the bottom of the wells containing the cells. After each incubation period, the medium was removed and the cell monolayer was washed twice with DPBS and fixed with 4% formaldehyde for 30 min. Subsequently, the formaldehyde solution was removed, and the cells washed with DPBS and the nuclei were stained with 4′,6-diamidino-2-phenylindole (DAPI). After incubation, DAPI solution was removed, and the cells were washed with DPBS and observed by fluorescence microscope. The images were recorded using an Axio Cam MRm (Zeiss).

2.10. Statistical analysis

A one way analysis of variance (ANOVA) was applied to compare different groups. Data were considered statistically significant with a value of $P < 0.05$ and differences between the groups were compared using a posteriori Bonferroni *t*-test. All values are the average of three experiments ± standard deviation.

3. Results and discussion

3.1. Synthesis of inulin-graft co-polymers

INU-Sq-PEG_{2000} is an amphiphilic polysaccharide based graft-copolymer useful for the preparation of self-assembled nanocarriers or as coating material of colloidal nanoparticles. In a previously published article [6], a similar copolymer carrying ceramide tails have been already studied for the preparation of polymeric micelles. Herein, being hydrophobic interactions useful only to stabilize the polymeric coating by the London dispersion forces, the synthesis of this copolymer was basically adapted in order to obtain a copolymer bearing squalenoyl branches as biocompatible hydrophobic moieties, conferring appropriate hydrophobicity still maintaining a good biocompatibility.[34]

Inulin (α-D-glucopyranosyl-[β-D-fructofuranosyl](*n*-1)-D-fructofuranoside), a linear polysaccharide consisting of glucopyranose end-capped fructose units (β-1,2), was used as main biocompatible polymeric backbone. First of all, it was partially functionalized with EDA so as to introduce primary

amine pendants that can be utilized as versatile functional groups allowing further functionalization [6]. A derivatization degree in EDA of 28% was obtained (DD_{EDA}, 28 mol%, related to inulin monomer units).

A squalene derivative (SqCOOH-C_{27}) carrying a carboxylic functional group available for additional coupling reactions was synthesized starting from 1,1′,2-tris-nor-squalene aldehyde. After the usual work-up, SqCOOH-C_{27} was obtained in 35% yield. From the ^{1}H NMR analysis, the presence of a characteristic signal of the carboxylic acid at 12.20 ppm, along with the observation of a shift of the vicinal hydrogens (CH_2CH_2COOH) observed at 2.26 ppm and 2.38 ppm respectively, confirmed the feasibility of the reaction. Furthermore, the molecular ion of the product (M+) observed at 400*m*/*z* by means of EI-MS analysis confirmed the hypothesis of the structure expected for the product.

In a second step, INU-EDA was functionalized with the squalenoyl derivative (SqCOOH-C_{27}) via amidic bond. In particular, SqCOOH-C_{27} was primarily activated using a mixture of EDC and NHS as coupling agents (Scheme 1). The stoichiometric conditions employed (moles of SqCOOH-C_{27}/moles of amino pendant groups in INU-EDA = 0.1; moles of EDC-HCl/moles of SqCOOH-C_{27} = 1.2 and moles of NHS/moles of SqCOOH-C_{27} = 1.2) were fixed to obtain a quantitative conversion of the SqCOOH-C_{27} carboxylic functions to amide.

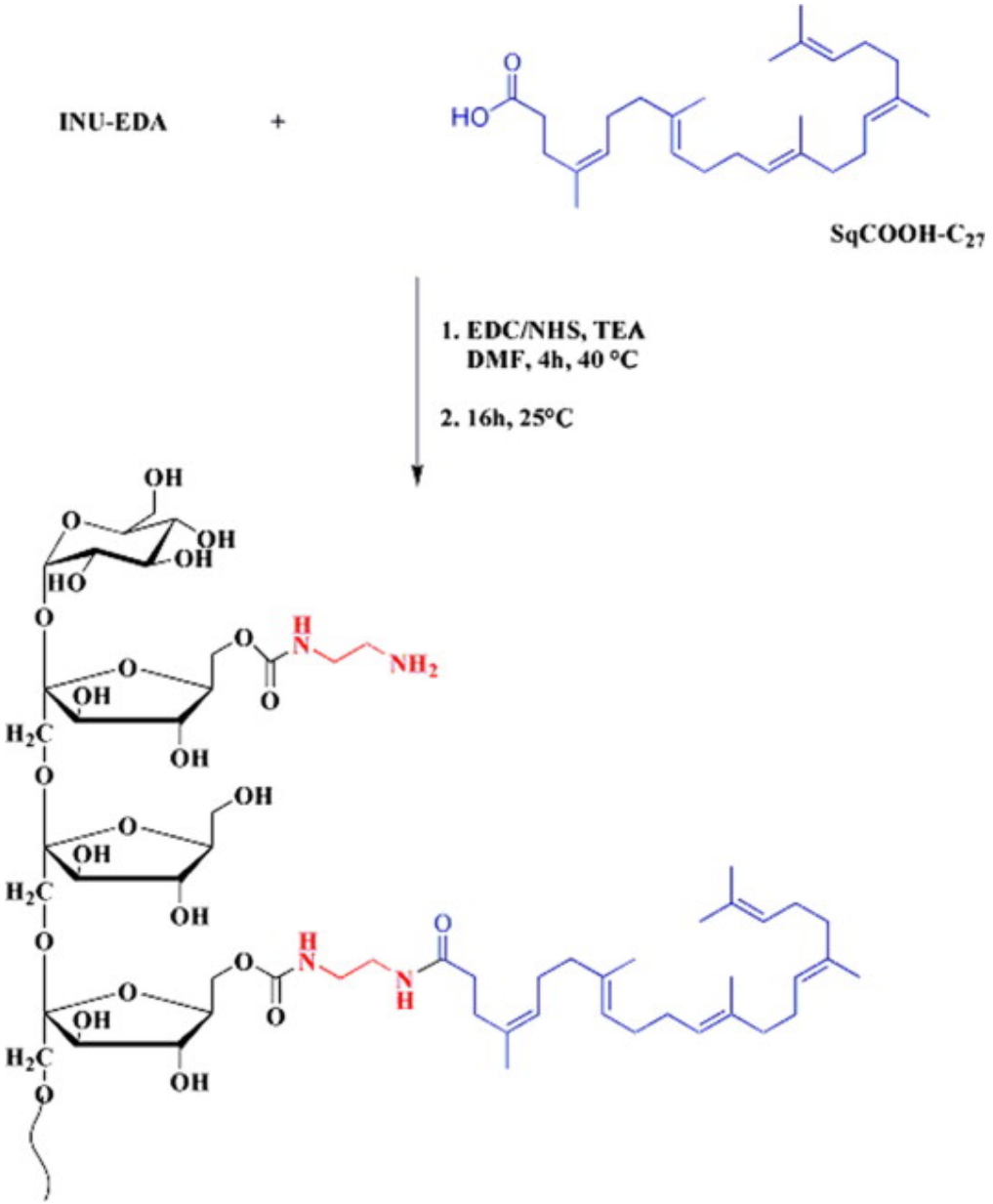

Scheme 1 - Synthesis of INU-Sq.

The ^{1}H NMR allowed an easy quantification of the SqCOOH-C_{27} linked to inulin, by comparing the integral of the peaks at δ 1.12–1.52 and at 1.91–2.21, ascribable to squalenoyl allylic CH_3 and allylic CH_2 respectively, to that belonging to the protons of INU backbone at δ comprised between 3.55 and 4.19. The molar percent of SqCOOH-C_{27}covalently linked to inulin (DD_{Sq}%) was equal to 1.7 ± 0.5 mol% referred to the inulin repeating units. The INU-Sq conjugates still maintain a large number of primary amine groups available for some potential subsequent side chain functionalization (about 90 mol% with respect to the total amount of amines), such as PEGylation. Hence, the last synthetic step was the synthesis of PEGylated INU derivative (INU-Sq-PEG_{2000}). In that reaction a semitelechelic aldehyde functionalized mono-methoxy PEG, having an weigh average molecular weight of 2000 Da, was selected to easily react in a slightly acidic aqueous medium with the primary amine groups available in the polymer side chain, yielding to the immine bounds (see Scheme 2).

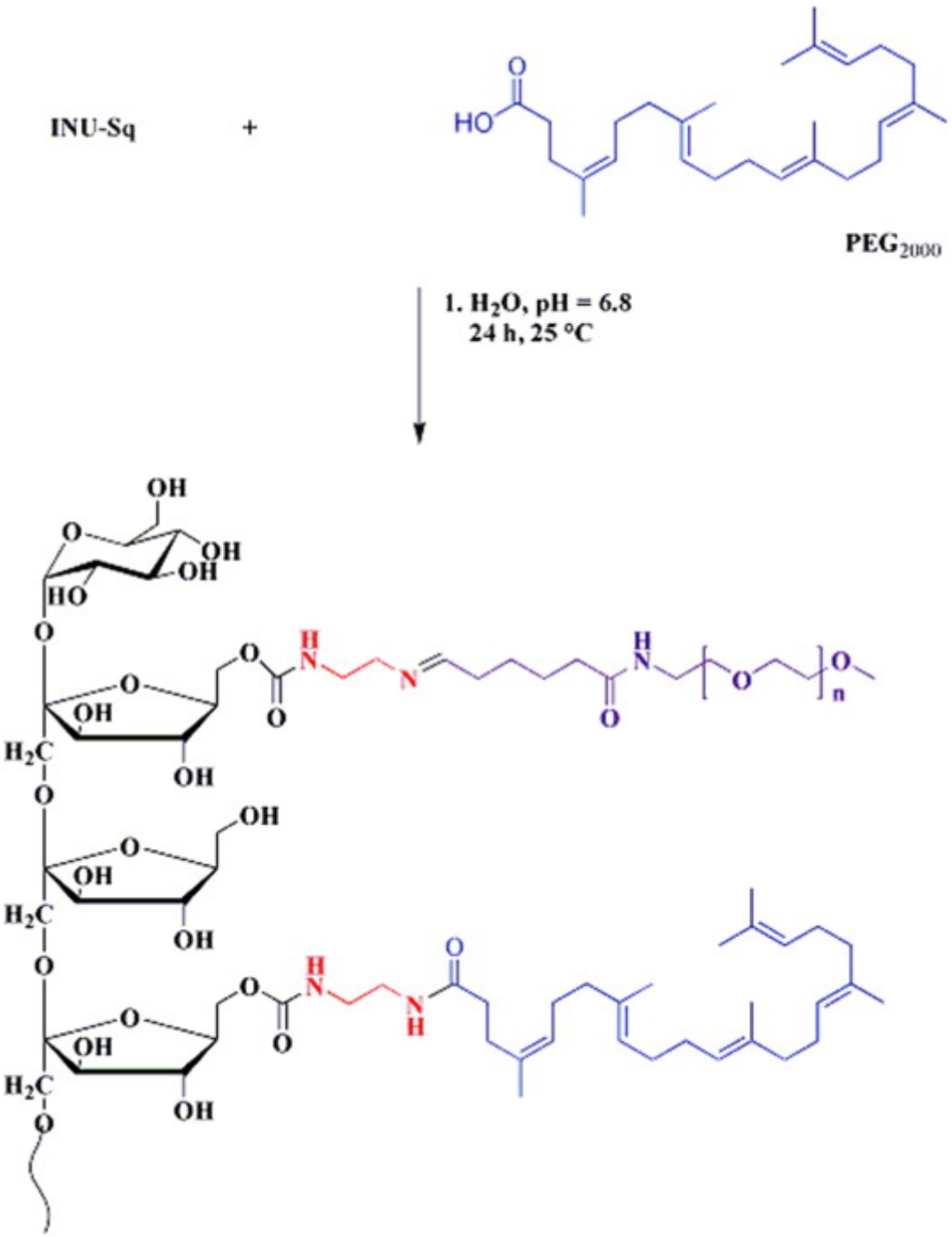

Scheme 2 - Synthesis of INU-Sq-PEG$_{2000}$ (n = 45).

INU-Sq-PEG$_{2000}$ copolymer was characterized by means of ^{1}H NMR spectroscopy, which confirmed the introduction of PEG$_{2000}$ chains on the INU-Sq backbone and allowed the calculation of the molar derivatization degree (DD$_{PEG}$%). The DD$_{PEG}$%, indicated as percentage of linked polyethylene chains in comparison with the repeating units of inulin, was calculated by comparing the integral of the peak related to protons at δ3.65 assigned to ethylene protons of PEG, with the integral of the peaks related to protons of INU backbone at δ comprised between 3.67 and 4.20. The DD$_{PEG}$% was equal to 2.7 ± 0.5 mol% referred to the inulin repeating units.

Weight average molecular weights (Mw) and polydispersity of the synthesized copolymers were determined by SEC analyses and data are reported in Table 1. The relative Mw of the polymers was obtained using a calibration curve of monodisperse pullulan standards with Mw ranging from 200 to 10,000. Definitively, the molecular weight increment of INU-Sq and INU-Sq-PEG_{2000} with respect to the starting INU-EDA copolymer confirm the derivatization of INU-EDA with Sq firstly and, subsequently, with PEG_{2000}. After the derivatization of inulin with EDA, a drastic molecular weight abatement was observed, passing from 4.9 kDa to 2.5 kDa. This might be ascribed to several factors. In first instance, conformational changes of the polymer chain, caused by the introduction of ionisable amine groups into the polymer backbone, imply variations in the hydrodynamic radii of the copolymers. On the other hand, microwave assisted reactions can entail the degradation of the main polymer chain, thus leading to a polymer with lower molecular weight [6]. Similar behavior was observed after the introduction of Sq moieties in the main backbone.

Table 1.

Molar derivatization degree values of EDA, Sq and PEG linked to inulin and molecular weight (Mw) and dispersity of the correspondent copolymers.

	Composition				
Copolymers	[a]$DD_{EDA\%}$	[a]$DD_{Sq\%}$	[a]$DD_{PEG\%}$	[b]Mw (kDa)	[b]Dispersity M_w/M_n
Inulin	–	–	–	4.9	1.3
INU-EDA	28 ± 1	–	–	2.5	1.8
INU-Sq	28 ± 1	1.7 ± 0.5	–	3.1	1.3
INU-Sq-PEG_{2000}	28 ± 1	1.7 ± 0.5	2.7 ± 0.5	4.3	1.2

a - Calculated by means of ^{1}H NMR spectroscopy

b - Calculated by SEC analysis.

3.2. Preparation and characterization of IC-SPIONs

Polymeric coated iron oxide nanoparticles were obtained adding INU-Sq-PEG_{2000}copolymer to iron oxide nanoparticles water dispersion dropwise. The simultaneous presence in the aqueous phase of both SPIONs, which are negatively charged (*Z*-potential = −29.2 ± 4 mV), and the cationic amphiphilic copolymers (*Z*-potential = +16 ± 5 mV) involves the adsorption of the latter on the surface of the iron oxide nanoparticle, thus acting as hydrocolloidal coating yielding to the stabilization of SPIONs in aqueous media. The drawing force that allows the IC-SPIONs formation is the ionic interaction established between SPIONs and INU-Sq-PEG_{2000} copolymer, as the Van der Waals interactions, with particular emphasis to the London dispersion forces, imply the assembling of the hydrophobic moieties of the amphiphiles adsorbed onto the nanoparticles, which stabilize and consolidate the nano-aggregates.

Fig. 1 shows the morphology of IC-SPIONs obtained by high resolution SEM analysis. SEM micrographs showed a homogeneous spherical nanoparticles population and with a diameter of about 50 nm.

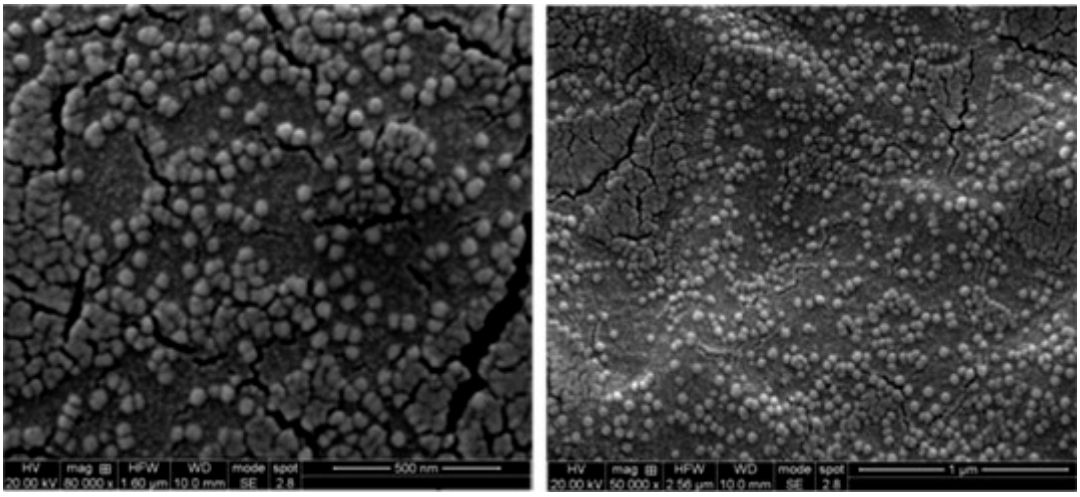

Fig. 1 - SEM images of IC-SPIONs.

These data were toughen up by DLS measurements which proved that the particle size observed by SEM have an average hydrodynamic diameter value of 54.79 nm and a PDI of 0.12 in aqueous dispersion as well. Zeta potential measures were also performed to establish the potential stability and polarity of the nanoparticles. It was found that the IC-SPIONs possessed positively charged surfaces with values of zeta potential of 21 ± 8 mV, probably due to the presence of protonated amines onto the nanoparticle surface. This value guarantees a good shelf stability of the system, along with the proper superficial charge helpful for the cellular up-take, which usually requires positively charged systems.

Doxorubicin loaded IC-SPIONs were then prepared to establish the ability of the system to act as a drug-delivery system. Doxorubicin was used as anticancer drug model because it is also endowed with fluorescence properties, which can be exploited to evaluate its uptake into cells by means of fluorescence microscopy. The drug loading procedure was carried out adding the aqueous doxorubicin hydrochloride solution, previously treated with TEA, to the polymer/Fe_3O_4 mixture. A molar excess of TEA was added to drug solution in order to obtained doxorubicin free base, with a less water solubility, so becoming more affine to the hydrophobic portion of the coating consisting of the squalenoyl tails. The amount of drug loaded evaluated by UV analysis was found to be 11.6 ± 0.5% (w/w), while the encapsulation efficiency was calculated to be 58.5%. DLS measurements carried out on Doxo-IC-SPIONs showed a reduction in size upon doxorubicin loading into nanoparticles, perhaps due to the formation of hydrophobic domains consisting of Sq moieties and aromatic portions of doxorubicin. Such interactions also explain well the higher polydispersity observed for the Doxo-IC-SPIONs (see Table 2). Being hydrophobic interactions concentration dependent phenomena, during the first step nanoparticles had available a large number of doxorubicin molecules which gave rise to compacted nanoparticles with high drug payload. After drug dilution, lesser drug–Sq interactions brought about bigger nanoparticles with a lower payload thus yielding to a high polydisperse system. As the lack of significant *Z* potential variations, which affects nanoparticles surface, endorsed the hypothesis that all changes provoked by doxorubicin involved the Doxo-IC-SPIONs core.

Table 2. - DLS data and zeta potential values of IC-SPIONs and Doxo-IC-SPIONs samples in aqueous medium at a final copolymer concentration of 0.2 mg/mL.

Sample	Hydrodynamic diameter (nm)	PDI	Zeta potential (mV)
IC-SPIONs	54.19	0.16	21 ± 8
Doxo-IC-SPIONs	44.15	0.46	19.8 ± 2

The chemical composition of the hybrid nanoparticles, that is Doxo-IC-SPIONs and IC-SPIONs, was assessed by ferrozine colorimetric iron determination assay and for the latter also by FTIR spectroscopy. The total iron oxide amount in IC-SPIONs and Doxo-IC-SPIONs is revealed by the ferrozine assay, and was found to be equal to 6.5 ± 1% and 7.7 ± 1% on a weight basis respectively. The existence of the polymer coating on the IC-SPIONs surface was further investigated by FTIR analysis. In Fig. 2 the spectra are reported in comparison with Fe_3O_4 and INU-Sq-PEG_{2000} copolymer alone. The IR spectrum of Fe_3O_4 showed only the characteristic broad band of Fe—O stretching at 579 cm^{-1}, whereas the INU-Sq-PEG_{2000} copolymer displays characteristic stretching bands of carbonyl functions at about 1650 and 1740 cm^{-1}, coupled with some broad bands at 1100 cm^{-1}, together with typical bands in the region of 1500–1200 cm^{-1}. The spectrum of IC-SPIONs clearly showed the vibrating bands of the polymer consistent with the existence of a polymer coating on magnetite core.

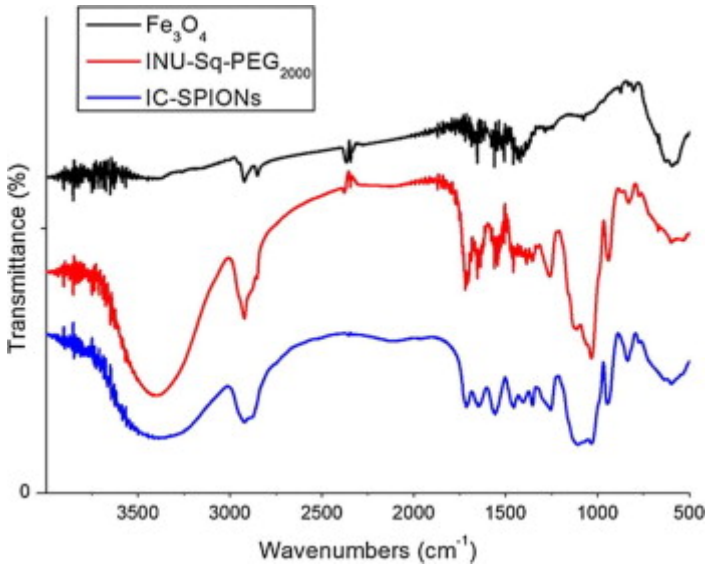

Fig. 2. - FTIR spectra of magnetite (Fe_3O_4), INU-Sq-PEG_{2000} copolymer and IC-SPIONs. (For interpretation of the references to color in this figure legend, the reader is referred to the web version of this article.)

The superparamagnetic behavior of prepared IC-SPIONs was already evidenced macroscopically by the effect of an external magnetic field on their water dispersion. InFig. 3, photograph of IC-SPIONs dispersion is shown (a), clearly displaying that nanoparticles are well dispersed throughout the sample. It can be noticed that, after the application of an external magnetic field for some minutes,

nanoparticles moved toward the magnet (b), whereas a homogeneous dispersion was obtained after the removal of the magnetic stimulus (c).

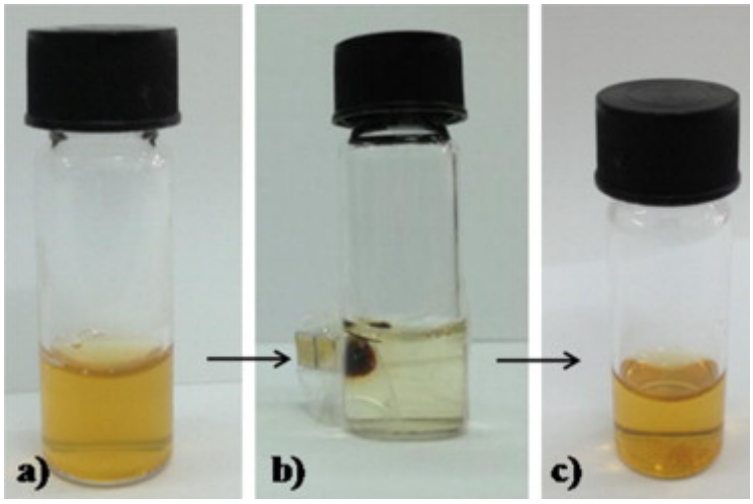

Fig. 3. - Photographs of IC-SPIONs water dispersion before (a) during (b) and after (c) the application of an external magnetic field overnight. (For interpretation of the references to color in this figure legend, the reader is referred to the web version of this article.)

3.3. Drug release studies

To evaluate the capability of Doxo-IC-SPIONs to release the loaded model drug, release experiments were carried out in two media simulating different human body compartments. In particular, PBS solution at pH 7.4, which mimics physiological medium (Fig. 4a) and pH 5.5, mimicking endosomal and lysosomal environments were used (Fig. 4b). The release experiments at the two pH conditions consisted into quantify the amount of released doxorubicin in the external medium, at pre-determined time intervals and until 48 h. In Fig. 4a and b the amount of released doxorubicin, referred to the total amount of doxorubicin loaded into the micelles, is shown as function of the incubation time. The nanoparticles proved capable of releasing doxorubicin in the intact form for a prolonged period and without a first “burst effect”. For instance, after 48 h about 12% of doxorubicin payload was slowly released at the two pH conditions, providing good findings so as to guarantee the slow drug release once the site of action will be reached. Additionally, the release profile has not been affected by the pH of the medium.

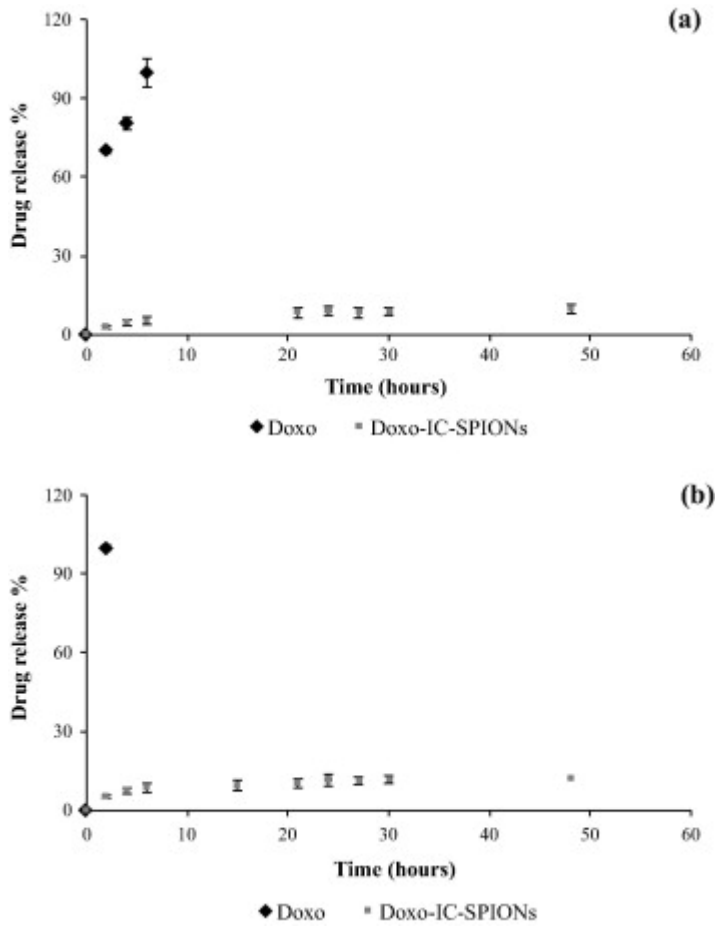

Fig. 4. - Drug release of Doxo-IC-SPIONs and doxorubicin hydrochloride in PBS solution at pH 7.4 (a) and at pH 5.5 (b).

3.4. In vitro biological evaluations

The effectiveness of the nanocarrier here prepared was established indirectly by evaluating the cytotoxicity of IC-SPIONs, Doxo-IC-SPIONs and doxorubicin hydrochloride on human colon cancer cells (HCT116), a cancer cell line used to investigate the anti-cancer activity of drugs and the associated mechanism of action [35], by MTS assay. MTS assay is based on the ability of mitochondrial dehydrogenases in viable cells to convert the MTS salt into a colored formazan product, which can be quantitatively detected by spectrophotometry at a λ_{max} of 490 nm. The obtained absorbance is directly proportional to the number of living cells in culture. In Fig. 5 are reported the cytotoxicity profiles at 24 h and 48 h of incubation time of the plain drug at concentration in the range of 25–200 µM (5a), IC-SPIONs at concentration within the range 0.13–1.08 mg/mL (5b), and Doxo-IC-SPIONs (5c) at the same concentration above reported for IC-SPIONs, corresponding to the amount the doxorubicin tested in the positive control (5a). Fig. 5a shows that doxorubicin alone displayed a dose-dependent cytotoxicity profile passing from 32% of cell viability at the concentration of 25 µM to 0% at the concentration of 200 µM and 48 h of incubation.

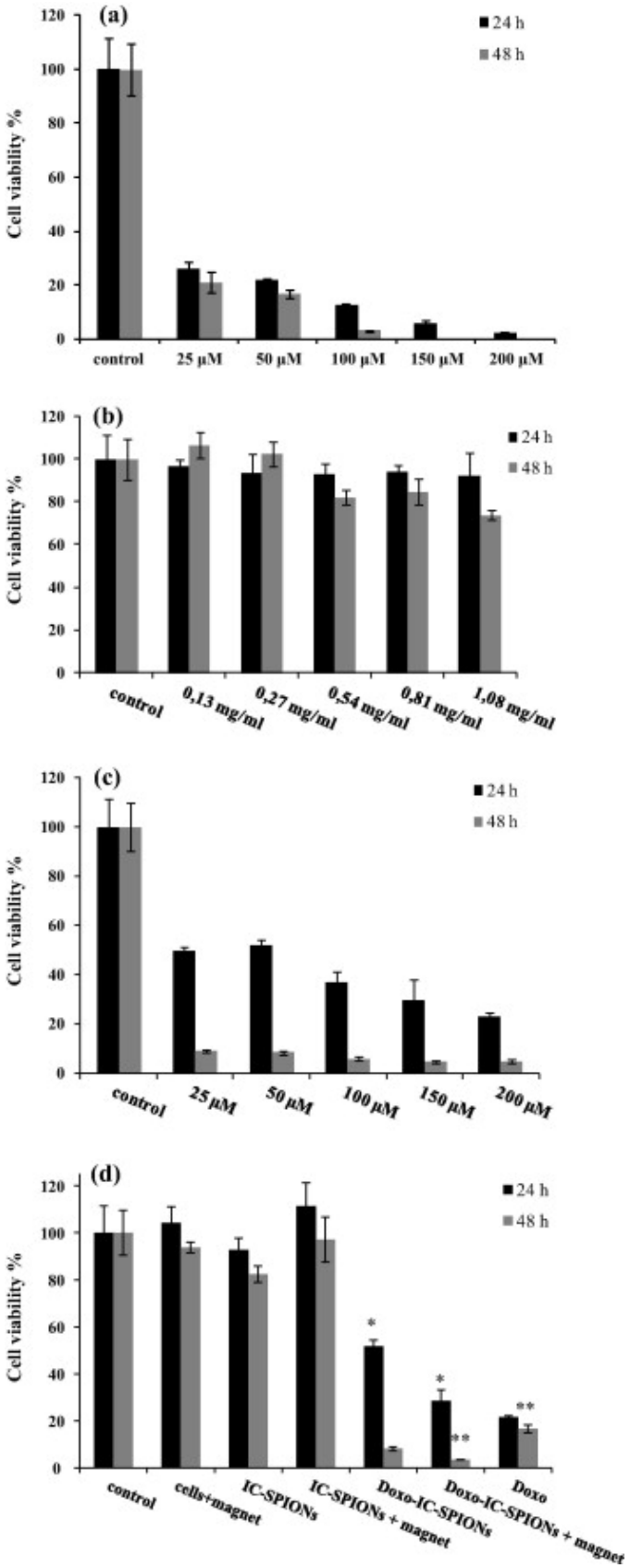

Fig. 5. - Cell viability % (MTS assay) on colon cancer cells (HCT116) of: doxorubicin hydrochloride (a), IC-SPIONs (b), Doxo-IC-SPIONs (c) and all the samples previously mentioned in the presence and in the absence of the external magnet (d). Incubation times was 24 and 48 h. The results are reported as the mean ± SD (n = 6). $^{*}p$ = 0.0016, $^{**}p$ = 0.00018.

For IC-SPIONs, negligible effect and no significant differences both after 24 and 48 h in cell viability were detected, at the whole concentration range tested, with respect the untreated control, indicating a good cytocompatibility of the empty system (Fig. 5b).

While, the cytotoxicity profile obtained for increasing dose of Doxo-IC-SPIONs makes viewable a quasi-dose-independent trend of effectiveness (Fig. 5c), in particular after 48 h of incubation. The variation in cytotoxicity observed at different concentration was indeed within range of standard errors. Worthy of note is that the cytotoxicity observed after 48 h is higher than that revealed after 24 h of incubation, thus suggesting that nanoparticles provide an intracellular reservoir of the drug, which is gradually released and internalized within nuclei. Moreover, even at the lower dosage, namely at 25 and 50 μM, the activity observed for Doxo-IC-SPIONs was remarkable higher, after 48 h of incubation, if compared with the same dose of plain drug, varying from 9% and 8% (Fig. 5c) to 20% and 16% (Fig. 5a) of viability respectively. This behavior clearly confirms that the loaded drug was locally and efficiently internalized into the cytosol compartment and there slowly released. Differently, free doxorubicin is rapidly internalized but also promptly expelled from the above compartment by the activation of the cell drug resistance mechanism, such as, for instance, those due to the efflux pump activity [36].

The same experiment was performed applying a permanent magnetic field at the bottom of the wells as shown in Fig. 5, in order to evaluate the effect of the magnetic field on cells viability.

In particular, IC-SPIONs at concentration of 0.27 mg/mL and Doxo-IC-SPIONs at the same concentration, which corresponds to 50 μM in doxorubicin hydrochloride, were incubated for 24 h and 48 h either in the presence of a magnetic field or not. Results are reported in Fig. 5d with respect to cells treated with the magnetic field alone and cells treated with doxorubicin hydrochloride at concentration of 50 μM. All results are reported as function of the control, which is the cell viability of untreated cells. As can be seen from the Fig. 5d, the magnetic field applied both to the untreated cell culture and the cells treated with the IC-SPIONs did not affect cell viability, since the cell viability was definitely comparable to that of the control. As, the cytotoxic effect on HCT116 cells increases by about 50% when cells were incubated with Doxo-IC-SPIONs for 24 h in the presence of the external magnet, while the effectiveness was lower if compared with the same dose of free doxorubicin hydrochloride. On the other hand, the persistence of the external field for 48 h enhanced the effectiveness of the Doxo-IC-SPIONs (3.4 ± 0.1% of viability observed), being extensively higher than that expressed by the same dose of free doxorubicin hydrochloride (16.6 ± 1.7% in Fig. 5a). These results prove that the attractive force of the magnetic field on the magnetic particles that increase the particles penetration into cells [17] and [37], in combination with the slow drug release into cells above discussed, aids to an important improvement of the anticancer activity of doxorubicin.

Finally, the ability of IC-SPIONs to release doxorubicin payload into HCT116 cells was confirmed by fluorescence microscopy analysis, incubating HCT116 cells with Doxo-IC-SPIONs, at drug concentration of 50 μM, both with and without the application of the external magnetic field. Fig. 6 shows the image of cells after 4 (a), 24 (b) and 48 h (c) of incubation. These studies showed that free doxorubicin was rapidly accumulated in HCT116 nuclei just after 4 h of incubation (see line A of Fig. 6a), and no substantial differences in intracellular trafficking were observed after 24 and 48 h,

apart from the reduction of live cells (line A of Fig. 6b and c). Differently, in the case of Doxo-IC-SPIONs incubated without the external magnet, the higher fluorescence intensity is visualized in the cell cytoplasm after 4 h of incubation (see line B of Fig. 6a). The same result was obtained with Doxo-IC-SPIONs incubated with the external magnet (see line C of Fig. 6a). After 24 h of incubation, a diffuse red fluorescence appeared inside cell nuclei also in cells treated with Doxo-IC-SPIONs (lines B and C of Fig. 6b), because doxorubicin was slowly released from nanoparticles. It is interesting to note that, in agreement with the cytotoxicity results above reported, the number of cells incubated with the external magnet appeared drastically reduced after 48 h of incubation (see line C of Fig. 6c), endorsing the hypothesis that the presence of the external magnetic force improves nanoparticles uptake. Moreover, it is well visible a red circle around the cell nuclei (see line C of Fig. 6c) presumably due to accumulation of Doxo-IC-SPIONs nanoparticle. This finding may confirmed the hypothesis that the magnetic force enhanced the Doxo-IC-SPIONs uptake and created a reservoir of the drug available inside cells that is slowly released into the nucleus, sustaining doxorubicin activity and eluding all possible drug resistance mechanisms.

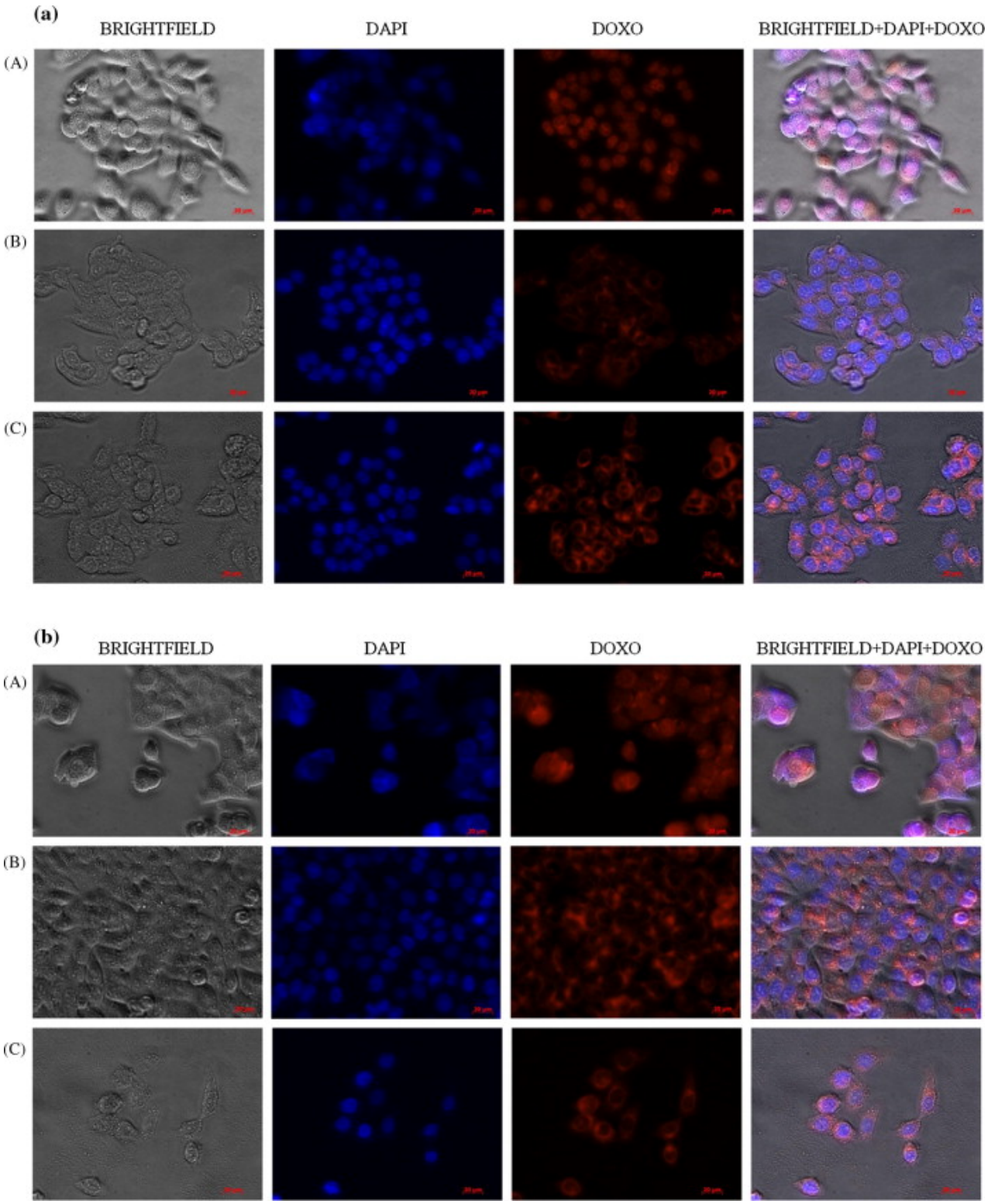
(a)
BRIGHTFIELD
DAPI
DOXO
BRIGHTFIELD+DAPI+DOXO
(A)
(B)
(C)
(b)
BRIGHTFIELD
DAPI
DOXO
BRIGHTFIELD+DAPI+DOXO
(A)
(B)
(C)

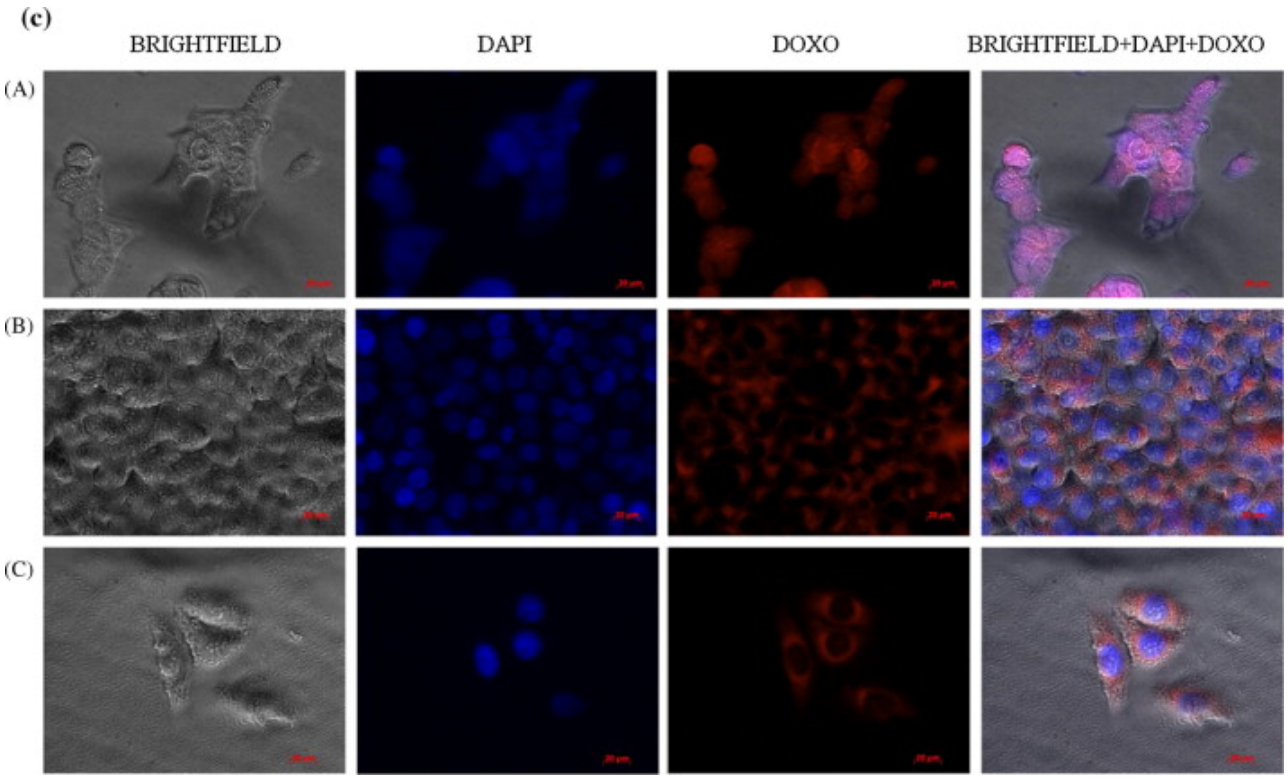

Fig. 6. - Fluorescence microscopy images of HCT116 cells incubated with free doxorubicin hydrochloride (line A), Doxo-IC-SPIONs (line B) and Doxo-IC-SPIONs with the application of the external magnet (line C). incubation times were 4 (panel a), 24 (panel b) and 48 h (panel c). Doxorubicin (DOXO) is visualized in red; cell nuclei were stained with DAPI (blue). Magnification is 40× for all images. (For interpretation of the references to color in this figure legend, the reader is referred to the web version of this article.)

4. Conclusions

In this work, the synthesis of squalene-grafted-inulin copolymer bearing PEG_{2000}moieties to give an amphiphilic copolymer with stealth like behavior is reported. This copolymer was easily obtained by in turn conjugating squalenoyl derivative and semitelechelic aldehyde terminated PEG chains of average weight molecular weight 2000, without employing drastic synthetic conditions. The introduction of squalenoyl tails in the hydrophilic backbone allowed obtaining a copolymer able to self-assemble into organized shell, once incubated with superparamagnetic iron oxide nanoparticles (SPIONs), leading to stable polymer coated SPIONs with average diameter of about 50 nm. We demonstrated that, in the presence of an external magnetic field, the system is strongly accumulated into a specific area of cell culturing, displaying a good magnetic targeting. Besides, although the release rate of doxorubicin from the system at physiological conditions appeared limited and slow, the system showed higher anticancer activity if compared with doxorubicin alone, especially under the effect of a magnetic field. On the whole, we clearly display that magnetic targeting implies advantageous therapeutic effects, that is amplified drug uptake, potential suppression of side effects and, consequently, increased anticancer activity throughout the tumor mass.

Acknowledgements

We thank the MIUR, the University of Turin (Ricerca locale 2013-14) and University of Palermo (FFR 2012) for the financial support to this research.

References

[1] M.Z. Ahmad, S. Akhter, G.K. Jain, M. Rahman, S.A. Pathan, F.J. Ahmad, R.K. Khar.
Metallic nanoparticles: technology overview & drug delivery applications in oncology. Expert Opin. Drug Deliv., 7 (2010), pp. 927–942

[2] F. Si-Shen, S. Chien. Chemotherapeutic engineering: application and further development of chemical engineering principles for chemotherapy of cancer and other diseases. Chem. Eng. Sci., 58 (2003), pp. 4087–4114

[3] S. Braunstein, L.J. Nakamura. Radiotherapy-induced malignancies: review of clinical features, pathobiology, and evolving approaches for mitigating risk. Front. Oncol. (2013), pp. 3–73

[4] E.S. Kawasaki, A. Player. Nanotechnology, nanomedicine, and the development of new, effective therapies for cancer. Nanomed.: Nanotechnol. Biol. Med., 1 (2005), pp. 101–109

[5] A. Kamb. Opinion: what's wrong with our cancer models? Nat. Rev. Drug Discov., 4 (2005), pp. 161–165

[6] M. Licciardi, C. Scialabba, C. Sardo, G. Cavallaro, G. Giammona. Amphiphilic inulin graft co-polymers as self-assembling micelles for doxorubicin delivery. J. Mater. Chem., 2 (2014), pp. 4262–4271

[7] E.F. Craparo, G. Teresi, M. Licciardi, M.L. Bondi', G. Cavallaro. Novel composed galactosylated nanodevices containing a ribavirin prodrug as hepatic cell-targeted carriers for hcv treatment. J. Biomed. Nanotechnol., 9 (2013), pp. 1107–1122

[8] D. Paolino, M. Licciardi, C. Celia, G. Giammona, M. Fresta, G. Cavallaro. Folate-targeted supramolecular vesicular aggregates as a new frontier for effective anticancer treatment in "in vivo" model. Eur. J. Pharm. Biopharm., 82 (2012), pp. 94–102

[9] J. Huwyler, J. Drewe, S. Krähenbühl. Tumor targeting using liposomal antineoplastic drugs. Int. J. Nanomed., 3 (2008), pp. 21–29

[10] W.H. Chiang, W.-C. Huang, C.-W. Chang, M.-Y. Shen, Z.-F. Shih, Y.-F. Huang, S.C. Lin, H.C. Chiue. Functionalized polymerosomes with outlayered polyelectrolyte gels for potential tumor-targeted delivery of multimodal therapies and MR imaging. J. Control. Release, 3 (2013), pp. 280–288

[11] Brannon-Peppas, J.O. Blanchette. Nanoparticle and targeted systems for cancer therapy. Adv. Drug Deliv. Rev., 56 (2004), pp. 1649–1659

[12] P.C. Griffiths, N. Mauro, D.M. Murphy, E. Carter, S.C.W. Richardson, P. Dyer, P. Ferruti. Self-assembled PAA-based nanoparticles as potential gene and protein delivery systems. Macromol. Biosci., 13 (2013), pp. 641–649

[13] H. Maeda, J. Wu, T. Sawa, Y. Matsumura, K. Hori. Tumor vascular permeability and the EPR effect in macromolecular therapeutics: a review. J. Control. Release, 65 (2000), pp. 271–284

[14] H. Maeda, T. Sawa, T. Konno. Mechanism of tumor-targeted delivery of macromolecular drugs, including the EPR effect in solid tumor and clinical overview of the prototype polymeric drug SMANCS. J. Control. Release, 74 (2001), pp. 47–61

[15] R.H. Kodama. Magnetic nanoparticles. J. Magn. Magn. Mater., 200 (1999), pp. 359–372

[16] L.W. Hamley. Nanotechnology with soft materials. Angew. Chem., 42 (2003), pp. 1692–1712

[17] J. Riemer, H.H. Hepken, H. Czerwinska, S.R. Robinson, R. Dringen. Colorimetric ferrozine-based assay for the quantitation of iron in cultured cells. Anal. Biochem., 331 (2004), pp. 370–375

[18] M. Licciardi, C. Scialabba, C. Fiorica, G. Cavallaro, G. Cassata, G. Giammona. Polymeric nanocarriers for magnetic targeted drug delivery: preparation, characterization, and in vitro and in vivo evaluation.
Mol. Pharmacol., 10 (2013), pp. 4397–4407

[19] M. Mahmoudi, S. Santc, B. Wang, S. Laurent, T. Sen. Superparamagnetic iron oxide nanoparticles (SPIONs): development, surface modification and applications in chemotherapy. Adv. Drug Deliv. Rev., 63 (2011), pp. 24–46

[20] L. Zhang, F. Gong, F. Zhang, J. Ma, P. Zhang, J. Shen. Targeted therapy for human hepatic carcinoma cells using folate-functionalized polymeric micelles loaded with superparamagnetic iron oxide and sorafenib in vitro. Int. J. Nanomed., 8 (2013), pp. 1517–1524

[21] G.F. Li, J. Fan, R. Jiang, Y. Gao. Cross-linking the linear polymeric chains in the atrp synthesis of iron oxide/polystyrene core/shell nanoparticles. Chem. Mater., 16 (2010), pp. 1835–1837

[22] S.R. Wan, Y. Zheng, Y. Liu, H. Yan, K. Liu. Fe_3O_4 nanoparticles coated with homopolymers of glycerol mono(meth)acrylate and their block copolymers. J. Mater. Chem., 15 (2005), pp. 3424–3430

[23] M. van der Zee, J.H. Stoutjesdijk, P.A.A.W. van der Heijden, D. de Wit. Structure–biodegradation relationships of polymeric materials. 1. Effect of degree of oxidation on biodegradability of carbohydrate polymers. J. Environ. Polym. Degrad., 3 (1995), pp. 235–242

[24] S. Kolida, G.R. Gibson. Prebiotic capacity of inulin-type fructans. J. Nutr., 137 (2007), pp. 2503S–2506S

[25] G. Pitarresi, D. Triolo, M. Giorgi, C. Fiorica, F. Calascibetta, G. Giammona. Inulin-based hydrogel for oral delivery of flutamide: preparation, characterization, and in vivo release studies. Macromol. Biosci., 12 (2012), pp. 770–778

[26] E.F. Craparo, G. Cavallaro, M.L. Bondi, D. Mandracchia, G. Giammona. Pegylated nanoparticles based on a polyaspartamide. Preparation, physico-chemical characterization, and intracellular uptake. Biomacromolecules, 7 (2006), pp. 3083–3092

[27] D. Mandracchia, G. Tripodo, A. Latrofa, R. Dorati. Amphiphilic inulin-d-rmalpha-tocopherol succinate (invite) bioconjugates for biomedical applications. Carbohydr. Polym., 103 (2014), pp. 46–54

[28] F.S. Palumbo, G. Pitarresi, D. Mandracchia, G. Tripodo, G. Giammona. New graft copolymers of hyaluronic acid and polylactic acid: synthesis and characterization. Carbohydr. Polym., 66 (3) (2006), pp. 379–385

[29] J. Ren, P. Wang, F. Dong, Y. Feng, D. Peng, Z. Guo. Synthesis and antifungal properties of 6-amino-6-deoxyinulin, a kind of precursors for facile chemical modifications of inulin. Carbohydr. Polym., 87 (2012), pp. 1744–1748

[30] J. Ren, J. Liu, F. Dong, Z. Guo. Synthesis and hydroxyl radicals scavenging activity of N-(aminoethyl)inulin. Carbohydr. Polym., 85 (2011), pp. 268–271

[31] M. Ceruti, F. Rocco, F. Viola, G. Balliano, G. Grosa, F. Dosio, L. Cattel. Synthesis and biological activity of 19-azasqualene 2,3-epoxide as inhibitor of 2,3-oxidosqualene cyclase. Eur. J. Med. Chem., 28 (1993), pp. 675–682

[32] Cattel, M. Ceruti, G. Balliano, F. Viola, G. Grosa, F. Rocco, P. Brusa. 2,3-Oxidosqualene cyclase: from azasqualenes to new site-directed inhibitors. Lipids, 30 (1995), pp. 235–246

[33] F. Viola, M. Ceruti, L. Cattel, P. Milla, K. Poralla, G. Balliano. Rationally designed inhibitors as tools for comparing the mechanism of squalene-hopene cyclase with oxidosqualene cyclase. Lipids, 35 (2000), pp. 297–303

[34] P. Couvreur, L.H. Reddy, B. Pili, C. Bourgaux, M. Ollivon. Discovery of new hexagonal supramolecular nanostructures formed by squalenoylation of an anticancer nucleoside analogue. Small, 4 (2) (2008), pp. 247–253
[35] G. Pitarresi, F.S. Palumbo, A. Albanese, C. Fiorica, P. Picone, G. Giammona. Self-assembled amphiphilic hyaluronic acid graft copolymers for targeted release of antitumoral drug. J. Drug Targeting, 18 (2010), pp. 264–276
[36] F. Shen, S. Chu, A.K. Bence, B. Bailey, X. Xue, P.A. Erickson, M.H. Montrose, W.T. Beck, L.C. Erickson. Quantitation of doxorubicin uptake, efflux, and modulation of multidrug resistance (MDR) in MDR human cancer cells. J. Pharmacol. Exp. Ther., 324 (2008), pp. 95–102
[37] V. Sundaresana, J.U. Menon, M. Rahimi, K.T. Nguyena, A.S. Wadajkar. Dual-responsive polymer-coated iron oxide nanoparticles for drug delivery and imaging applications. Int. J. Pharm., 466 (2014), pp. 1–7